

Retraction

Retracted: A Research on the Control System of High-Speed Homopolar Motor with Solid Rotor Based on Flywheel Energy Storage

Complexity

Received 23 January 2024; Accepted 23 January 2024; Published 24 January 2024

Copyright © 2024 Complexity. This is an open access article distributed under the Creative Commons Attribution License, which permits unrestricted use, distribution, and reproduction in any medium, provided the original work is properly cited.

This article has been retracted by Hindawi following an investigation undertaken by the publisher [1]. This investigation has uncovered evidence of one or more of the following indicators of systematic manipulation of the publication process:

- (1) Discrepancies in scope
- (2) Discrepancies in the description of the research reported
- (3) Discrepancies between the availability of data and the research described
- (4) Inappropriate citations
- (5) Incoherent, meaningless and/or irrelevant content included in the article
- (6) Manipulated or compromised peer review

The presence of these indicators undermines our confidence in the integrity of the article's content and we cannot, therefore, vouch for its reliability. Please note that this notice is intended solely to alert readers that the content of this article is unreliable. We have not investigated whether authors were aware of or involved in the systematic manipulation of the publication process.

Wiley and Hindawi regrets that the usual quality checks did not identify these issues before publication and have since put additional measures in place to safeguard research integrity.

We wish to credit our own Research Integrity and Research Publishing teams and anonymous and named external researchers and research integrity experts for contributing to this investigation.

The corresponding author, as the representative of all authors, has been given the opportunity to register their agreement or disagreement to this retraction. We have kept a record of any response received.

References

- [1] L. Jing, Y. Yu, and X. Xue, "A Research on the Control System of High-Speed Homopolar Motor with Solid Rotor Based on Flywheel Energy Storage," *Complexity*, vol. 2020, Article ID 6537563, 12 pages, 2020.

Research Article

A Research on the Control System of High-Speed Homopolar Motor with Solid Rotor Based on Flywheel Energy Storage

Lili Jing,¹ Yandong Yu ,² and Xiaochuan Xue³

¹Key Laboratory of High Speed Signal Processing and Internet of Things Technology Application, Jining Normal University, Ulanqab, Inner Mongolia 012000, China

²Department of Computer Science, Jining Normal University, Ulanqab, Inner Mongolia 012000, China

³Systems Engineering Research Institute of China State Shipbuilding Corporation, Beijing 100191, China

Correspondence should be addressed to Yandong Yu; cfssyyd@163.com

Received 17 April 2020; Revised 13 June 2020; Accepted 17 June 2020; Published 17 July 2020

Guest Editor: Zhihan Lv

Copyright © 2020 Lili Jing et al. This is an open access article distributed under the Creative Commons Attribution License, which permits unrestricted use, distribution, and reproduction in any medium, provided the original work is properly cited.

In view of the defects of the motors used for flywheel energy storage such as great iron loss in rotation, poor rotor strength, and robustness, a new type of motor called electrically excited homopolar motor is adopted in this paper for flywheel energy storage. Compared to general motors, this motor has the advantages of simple structure, high rotor strength, and low iron loss in rotation. A double closed-loop PI governing system of the new motor was designed, modeled, and simulated with this motor as the controlled object on simulation platform. The simulation result shows that the PI-controlled electrically excited homopolar motor system realized fast speed governing and good system performance, achieved the purpose of quick charge by flywheel energy storage, verified the correctness and effectiveness of the design scheme, and provided data reference and theoretical basis for the practice of future flywheel energy storage experiments.

1. Introduction

Today the whole world is confronted with an increasing shortage of energy. Besides, constantly developing new energies, how to utilize existing energies effectively has become a hot spot of people's attention. Energy storage is an important way to achieve efficient utilization of energy [1], so the storage technology of electric energy, as a main form of energy consumed today, has become the most important research subject in the energy field.

In the 21st century, flywheel energy storage, owing to its many advantages including high energy ratio, high power ratio, high efficiency, wide application, no pollution, no noise, easy maintenance, and long service life, is bound to bring about an evolution to energy storage and show the prospect of green energy storage technology [2]. In overseas, the research of flywheel energy storage technology started between 1950s and 1970s when magnetically levitated energy

storage flywheel was created in the form of a series of prototype. At present, international leading companies in the field of flywheel energy storage include US-based Active Power which produces and supplies with UPS and energy storage flywheel developed by Japanese company with HTS magnetic levitation technology, which is mainly used for the trolley bus. As a replacement of traditional energy technology, flywheel energy storage technology is applied to fields such as transportation, energy generation, and aerospace relying on its strong competitiveness. Now, China is relatively backward in this field and still in the fledging period, but is gradually emerging being impacted by the current great upsurge around the world. The Flywheel Energy Storage Laboratory of Tsinghua University was the first institution in China to initiate the research of this technology and developed an energy storage flywheel prototype in 1999, which laid a solid theoretical and experimental basis for our flywheel energy storage technology. In

addition, Beijing University of Aeronautics and Astronautics, Nanjing University of Aeronautics and Astronautics and North China Electric Power University, etc., also completed this technology experiment and obtained their unique patented products.

Flywheel energy storage is a kind of energy-storing device utilizing physical interconversion between electric energy and mechanical energy (kinetic energy). It is mainly composed of auxiliary devices including flywheel, flywheel motor, motor controller, bearings, and vacuum chamber [3]. The flywheel energy storage system completes energy absorption and release by the flywheel motor and its controller, so the flywheel motor is the main part of this device. Systems using different flywheel motors and control types may have different performances. The energy storage flywheel motor and its control system is a complex integrated electromechanical system. As a new type of motor, the homopolar motor has not been widely known yet. Due to its advantages such as simple structure, high-strength rotor, and low iron loss in high-speed rotation, it is especially suitable for energy storage flywheel. By modeling and simulation research of the high-speed control system of electrically-excited homopolar motor [4] as the controlled object, we aim to provide a preliminary theoretical foundation and essential experimental basis for the Research on Topology Optimization and Dynamically Decoupling Nonlinear Control of High-speed Permanent Magnet Homopolar Motor with Solid Rotor by NSF of Inner Mongolia, in order to save the design cost and R&D time.

2. Structure and Principle of Homopolar Motor

Electrically-excited homopolar motor, such as general motors, also consists mainly of rotor, stator, and other relevant components, as shown in Figure 1. The differences are the stator and rotor materials and structural design. Due to cost consideration, the rotor bearings choose angular contact ball bearings in order to ensure stable and high-speed operation. Its rotor is made of 40CrNiMoA, adopts high-strength forged solid-steel structure with flywheel-motor integrated design, and is designed with uniformly distributed concaves and convexes [5] and antisymmetric upper and lower ends, as shown in Figure 2. The flywheel-motor integrated design, which enables the rotor to integrate the functions of kinetic energy storage and electromagnetic force output, greatly simplifies the design process, reduces the production cost, and makes the solid-steel rotor; the flywheel has the same level of energy storage density as the composite rotor flywheel. Its stator is composed of two parts, the armature and the exciter; its section view is shown in Figure 3. The motor stator has such characteristics: its armature windings use tinned copper braid which is parallel to rotor length axis and evenly distributed along rotor circumference; currents in adjacent in-phase windings flow to opposite directions; and three-phase current generates space rotating magnetic field; while the salient pole of the rotor induced by electromagnetic force drives the motor to rotate. The motor's parameters are provided in Table 1.

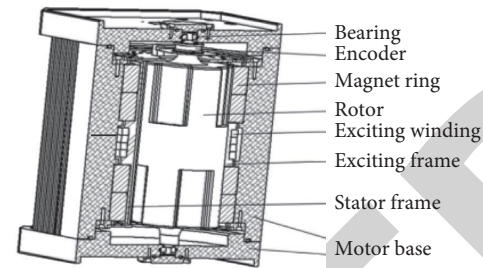


FIGURE 1: Section of motor assembly.

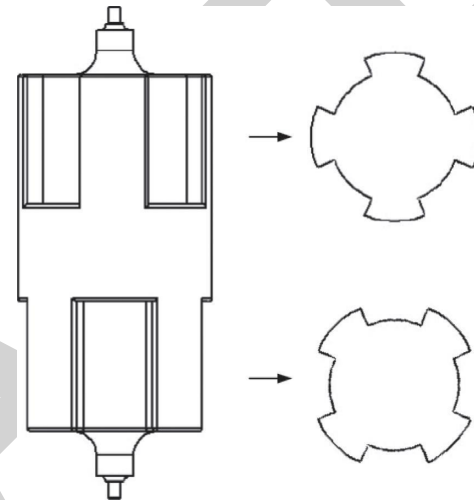


FIGURE 2: Structure of solid rotor.

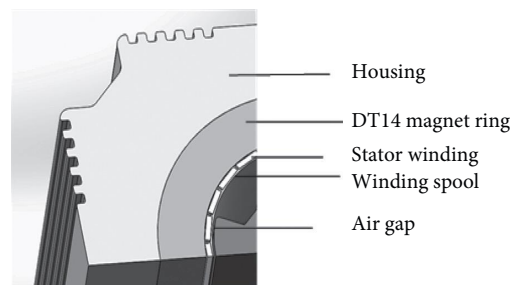


FIGURE 3: Section of stator.

Running principle of electrically excited homopolar motor; its space magnetic field is generated by the impressed current through the exciting windings around the end circumference. Its magnetic loop is a closed circuit formed by exciting flux flowing from the upper end of the rotor, through the magnet ring and air gap into the lower end. Because the rotor's magnetism is generated by the exciting coil, its magnetic strength is controllable by exciting current. The motor rotates as its rotor's salient pole senses the corresponding space rotating magnetic field, while the required space rotating magnetic field is generated by the variable three-phase current through the rotor. The motor's operational principle is shown in Figures 4 and 5. As stator current flows from A to C, seen from the motor's upper end in Figure 4, A-phase winding current flows

TABLE 1: Parameters of electrically excited homopolar motor.

Motor parameters	Rotor parameters		Stator parameters		Exciting parameters		
Housing material	6063-t5	Rotor material	40CrNiMoA	Armature material	VF wire	Magnet ring material	DT4-E
Magnetic gap	4.0 mm	Diameter	90 mm	Winding diameter	1.82 mm	Magnetic conductivity	0.0113H·m ⁻¹
Housing volume	200 × 200 × 230 mm ³	Length	213 mm	Stator turns	10	Coil turns	1250
Gross mass	19 kg	Rotor mass	5.98 kg	Rated current	10.4 A	Coil current	<2 A

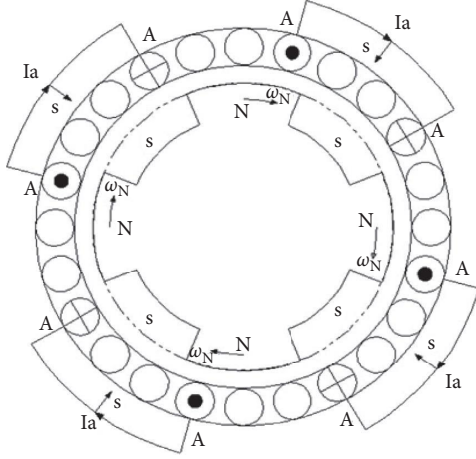


FIGURE 4: Upper stator and rotor of the motor.

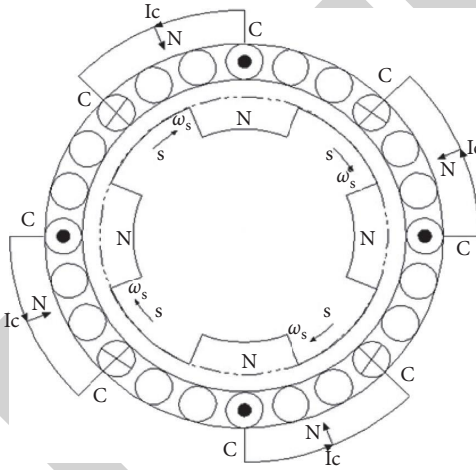


FIGURE 5: Lower stator and rotor of the motor.

clockwise; the magnetic field generated by armature winding is inward at S pole and outward at N pole. The upper salient pole (N pole) of the rotor rotates clockwise when induced by this electromagnetic force; similarly and simultaneously, seen from the motor's lower end in Figure 5, the rotor's salient pole (S pole) also rotates clockwise being driven by the magnetic field generated by the current varying counterclockwise in C-phase winding, i.e., the rotating magnetic field produced by variable current in the motor stator acts on the motor rotor and drives the latter to rotate.

3. Mathematical Model of Homopolar Motor

As the rotor of the motor in this paper has the characteristics of the salient pole structure, we built and deduced a unified dynamic mathematical model [6, 7] of the motor in the stator's three-phase coordinate system based on the basic electromagnetic relationship. And because the counter electromotive force wave and phase current output by the motor are similar to those by brushless DC motor, this motor's mathematical model is approximate to that of brushless DC motor.

The mathematical model of electrically excited homopolar motor using the motor's own vector in the stator's three-phase coordinate system is shown in Figure 6.

In this figure as , bs , and cs are the corresponding axes of three-phase stator windings; $A-A'$, $B-B'$, and $C-C'$ are three-phase stator windings; the rotor speed ω_r is set as counterclockwise, ψe is the flux linkage vector generated by the external electromagnetic, forming an angle of α with the plane of the stator three-phase coordinate system; and ψe_0 is the projection of ψe in the coordinate system plane, with an angle of θ with axis as .

Without affecting the control performance, simplified analysis shows that three-phase windings of the motor are symmetric, and its stator's voltage state equation is as follows:

$$\begin{bmatrix} u_a \\ u_b \\ u_c \end{bmatrix} = \begin{bmatrix} R_a & 0 & 0 \\ 0 & R_b & 0 \\ 0 & 0 & R_c \end{bmatrix} \begin{bmatrix} i_a \\ i_b \\ i_c \end{bmatrix} + \begin{bmatrix} L_a & L_{ab} & L_{ac} \\ L_{ba} & L_b & L_{bc} \\ L_{ca} & L_{cb} & L_c \end{bmatrix} \frac{d}{dt} \begin{bmatrix} i_a \\ i_b \\ i_c \end{bmatrix} + \begin{bmatrix} e_a \\ e_b \\ e_c \end{bmatrix}. \quad (1)$$

In this equation, u_a , u_b , and u_c are, respectively, the stator's three-phase terminal voltages (V); R_a , R_b , and R_c are the resistances (Ω) of the motor's three-phase windings; L_{ab} , L_{ba} , L_{ca} , L_{ac} , L_{bc} , and L_{cb} are the mutual inductances (H) among the three-phase stator windings; L_a , L_b , and L_c are the self-inductances (H) of the motor's three-phase windings; e_a , e_b , and e_c are, respectively, the counterelectromotive forces (V) of the motor's three-phase windings; and i_a , i_b , and i_c are the three-phase currents (A) of the stator.

Assuming that the three-phase winding is symmetric and the reluctance of rotor does not change as the rotor position shifts.

Namely, $R = R_a = R_b = R_c$, $M = L_{ab} = L_{ac} = L_{bc} = L_{ba} = L_{ca} = L_{cb}$, and $L = L_a = L_b = L_c$.

In the brushless DC motor, the three-phase winding is symmetric; then,

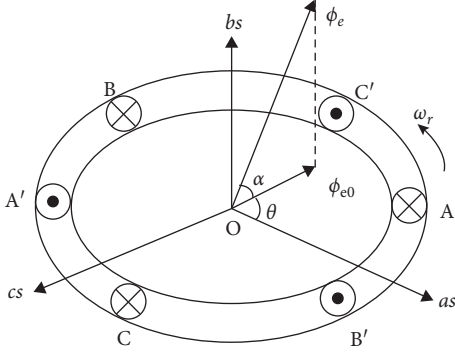


FIGURE 6: Mathematical model of motor's 3-phase stator.

$$i_a + i_b + i_c = 0, \quad (2)$$

$$Mi_a + Mi_b + Mi_c = 0. \quad (3)$$

Thus, from equation (1), we can deduce

$$\begin{bmatrix} u_a \\ u_b \\ u_c \end{bmatrix} = \begin{bmatrix} R & 0 & 0 \\ 0 & R & 0 \\ 0 & 0 & R \end{bmatrix} \begin{bmatrix} i_a \\ i_b \\ i_c \end{bmatrix} + \begin{bmatrix} L-M & 0 & 0 \\ 0 & L-M & 0 \\ 0 & 0 & L-M \end{bmatrix} \frac{d}{dt} \begin{bmatrix} i_a \\ i_b \\ i_c \end{bmatrix} + \begin{bmatrix} e_a \\ e_b \\ e_c \end{bmatrix}. \quad (4)$$

The flux-linkage equation of the homopolar motor stator in the three-phase coordinate system is as follows:

$$\begin{cases} \psi_A = L_A i_A + M_{AB} i_B + M_{AC} i_C + \psi_e \cos \alpha \cos \theta, \\ \psi_B = L_B i_B + M_{AB} i_A + M_{BC} i_C + \psi_e \cos \alpha \cos \left(\theta + \frac{2}{3} \pi \right), \\ \psi_C = L_C i_C + M_{AC} i_C + M_{BC} i_B + \psi_e \cos \alpha \cos \left(\theta + \frac{4}{3} \pi \right). \end{cases} \quad (5)$$

The equation of the electromagnetic torque generated by the interaction between impressed exciting field and stator current and the motor's motion equation is as follows:

$$T_e = \frac{(e_a i_a + e_b i_b + e_c i_c)}{\omega_r}, \quad (6)$$

$$J \frac{d\omega_r}{dt} = T_e - T_L - B\omega_r. \quad (7)$$

In the equations, T_e is the motor's electromagnetic torque ($N \cdot m$); ω_r is the motor's mechanical angular velocity (rad/s); J is the motor's rotational inertia ($kg \cdot m^2$); T_L is the load torque ($N \cdot m$); and B is the damping coefficient (s^{-1}).

4. Control Strategy of Homopolar Motor

Famous scholar Astrom once said [8] "in process control today, more than 95% of the control loops are of PID type." It shows the dominance [9] of the PID controller in the field of process control. The flywheel energy storage motor control system focuses more on the motor's speed regulation time and less on indexes such as control precision. Therefore, PID strategy is used to control the double closed-loop system of the homopolar solid rotor motor and applied in the research on flywheel energy storage.

4.1. PID Control Strategy. PID control is the most commonly used control law in the simulation control system. It is a kind of linear controller. Its structure is shown in Figure 7. $r(t)$ is set input value; $e(t)$ is control deviation; $u(t)$ is control variable; and $y(t)$ is actual output value.

PID control law:

$$u(t) = K_p e(t) + \frac{K_p}{T_i} \int_0^t e(t) dt + K_p T_d \frac{de(t)}{dt}, \quad (8)$$

$$u(t) = K_p e(t) + K_i \int_0^t e(t) dt + K_d \frac{de(t)}{dt}. \quad (9)$$

In the form of transfer function,

$$G_s = \frac{U(s)}{E(s)} = K_p + \frac{K_p}{T_i s} + K_p T_d s, \quad (10)$$

or

$$G_s = \frac{U(s)}{E(s)} = K_p + \frac{K_i}{s} + K_d s. \quad (11)$$

In the equations above, K_p is proportionality coefficient; T_i is integral time constant; T_d is differential time constant; K_i is integral coefficient, $K_i = (K_p/T_i)$; and K_d is differential coefficient, $K_d = K_p \times T_d$.

For the convenience of computer implementation, the discrete method is adopted to convert continuous PID to the corresponding digital PID control algorithm [10, 11]. The expression is as follows:

$$u(k) = K_p e(k) + \frac{K_p T}{T_i} \sum_{j=0}^k e(j) + \frac{K_p T_d}{T} [e(k) - e(k-1)], \quad (12)$$

or

$$u(k) = K_p e(k) + K_i T \sum_{j=0}^k e(j) + \frac{K_d}{T} [e(k) - e(k-1)]. \quad (13)$$

In the equations, T is sampling period; k is sampling signal, ($k = 1, 2, 3, \dots$); $e(k)$ is system deviation input value at the k th time of sampling; $e(k-1)$ is system deviation input value at the $(k-1)$ th time of sampling; and $u(k)$ is control quantity output value at the k th time of sampling.

Its pulse transfer function is

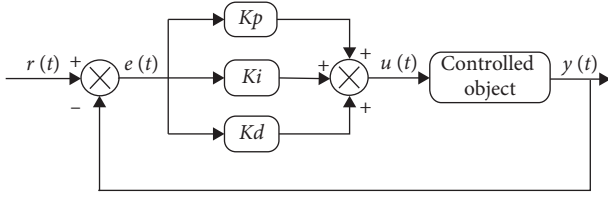


FIGURE 7: Block diagram of the PID controller.

$$G(z) = \frac{U(z)}{E(z)} = K_p + \frac{K_i T}{1 - z^{-1}} + \frac{K_d}{T} (1 - z^{-1}). \quad (14)$$

Commonly used digital PID control algorithms include the following:

- (1) Full PID control: this kind of control algorithm directly presents the execution point of the actuator (such as motor speed and valve opening), and thus it is named full variable or positional PID control algorithm. It directly calculates based on the defining equations (9) and (10) of PID control law. Its disadvantage is that the output is full variable and always associated with all past states; moreover, it requires accumulation of $e(k)$ in the calculation, which increases a huge amount of work.
- (2) Incremental PID control [11]: this control algorithm applies where the output is only the increment of the control variable. Where the actuator needs the increment of the controlled variable (such as step motor), incremental PID control algorithm can be deduced from full variable PID control algorithm. The formula is

$$\Delta U(k) = Ae(k) + Be(k-1) + Ce(k-2). \quad (15)$$

In this equation, $A = K_p + K_i T + (K_d/T)$; $B = K_p - (2K_d/T)$; and $C = (K_d/T)$

Once the sampling period and coefficients A , B , and C are determined, we can get the increment of the controlled variable by just entering three times of measurement deviations before and after the measurement. It presents the positional variation of the actuator between the two times of sampling. Compared with the positional one, the incremental one requires a much smaller amount of calculation and simple algorithm and is convenient for software programming. Therefore, it is widely used in practical production. Based on the incremental PID control algorithm, the recursion formula of full quantity PID control algorithm can also be deduced:

$$U(k) = U(k-1) + \Delta U(k). \quad (16)$$

The above formula is the digital recursive PID control algorithm widely used in digital control systems today.

Another great advantage of digital PID control is that it allows us to improve PID depending on the object and working condition so that PID control can achieve high-quality control effect in different fields. Commonly used improved digital PID control algorithms [12–15] include

differential forward PID control algorithm, incomplete differential control algorithm, integral clamping PID control algorithm, PID control algorithm with dead zone, and integral separation PID control algorithm.

4.2. PID Controller Tuning. We can see from PID control principle diagram 6 that the PID controller is composed of three major control links (proportion, integral, and differential) decided mainly by PID's three parameters which are mutually inseparable, interconnected, and restrictive. Look at the roles of proportion, integral, and differential in terms of overshoot, stability, response, and steady-state precision of the control system [10, 11]:

- (1) Proportional control link: proportionality coefficient K_p and deviation signal $e(t)$ together constitute the proportional control link. It is the most basic link and plays a leading role in PID control. Once deviation occurs to the system, this link is immediately activated to reduce deviation. However, proportional control alone cannot eliminate system deviation. There will be a residual error. Larger proportional control coefficient K_p means stronger control effect, faster system response, and higher stability precision, but a too large K_p value is easy to cause system overshoot, instability, and oscillation. On the contrary, a too small K_p will reduce system's stability precision, prolong the transition time for system to reach the set value, slow down its response time, and spoil system static and dynamic characteristics.
- (2) Integral control link: integral coefficient K_i and the time integral of deviation together constitute the integral control link. Its main function is to eliminate system static error and improve system stability. Larger K_i means faster speed of eliminating system static error, but a too large K_i value is easy to lead to overshoot at the beginning of control due to integral saturation. On the contrary, a too small K_i value will have little effect in eliminating system static error and will also reduce the system's control precision.
- (3) Differential control link: differential coefficient K_d and the time differential of deviation together constitute the differential control link. It compensates the function of the proportional control link, prevents system overshoot, suppresses oscillation, and maintains system stability. It mainly predicts deviation change in the process of response and reduces it. The K_d value should not be too large; otherwise, it will suppress the response process in advance, prolong the tuning time, and reduce the system's antiinterference performance.

From the above effects of proportional coefficient K_p , integral coefficient K_i , and differential coefficient K_d on system and the synergy of the three, we can see that they are all critical for system control. The parameters of the PID controller vary with the steady-state condition of the control system. Once the working condition (or the process object's "characteristic") changes, then the optimal value of the

controller parameter changes too. This means controller tuning may be necessary at any time so that the control system and process control object reach the required rapidity, precision, and stability [16]. Commonly used PID parameter tuning methods include the following.

Testing method parameter tuning is also called engineering tuning method. It applies the valuable experience people accumulated in long-term engineering practice to the control system to test directly. This method is simple and easy to grasp. The testing method is to find out characteristic parameters in the response system according to the testing result and work out the controlling parameter with empirical formula.

Attenuation curve methods include 4:1 attenuation curve method and 10:1 attenuation curve method.

Empirical method, also known as trial and error, is a PID parameter tuning method including three steps from proportion to integral and then to differential. Turn the parameters repeatedly according to this sequence until a desired effect is achieved. Here is the procedure. First, tune the value of the proportionality coefficient. Increase it one by one and find one with small overshoot and quick response. Now, observe whether there is a static error. Add the integral coefficient if there is. When tuning the integral coefficient, decrease the set value from large to small and at the same time tune the proportionality coefficient. Observe the system response until the system static error is eliminated. While the eliminating system static error, keep an eye on system overshoot and response time. If the system overshoot is very large or response is slow, add the differential coefficient and tune again until desired control effect is obtained.

5. Control System Design and Modeling

Flywheel energy-storage system is composed of three major parts, flywheel rotor, motor/generator, and controller. The controller, as the system command center, directly determines the system's control performance [17]. Therefore, in the process of designing the control system of high-speed homopolar solid rotor motor with energy-storing flywheel, we built a control system simulation model (Figure 8) of electrically excited homopolar motor based on its operation principle and mathematical model with the modular modeling method [18–20] on MATLAB/SIMLINK simulation platform in order to shorten the design cycle and lower the research cost and risk. The control system simulation model of homopolar motor consists of seven subsystems, including homopolar motor, inverter, speed controller PI-W1, current controller PI-current, PWM generator, commutator, and decoder, as well as speed reference w_r -ref and load module TL.

As energy-storing flywheel requires high motor efficiency, the system of this homopolar motor is designed with double-closed-loop control. The outer one is speed loop. It applies PI control strategy to its speed controller PI-W1 to ensure the system dynamic tracking performance and suppress speed fluctuation. The inner one is the current loop. It applies integral separation PI control strategy to its current controller PI-current to limit the maximum current, makes

the system have enough accelerating torque, and ensures system stability and high-performance operation. Signal from the current controller is sent into the PWM generator which then produces PWM signal with adjustable pulse width. Then, PWM signal, along with rotor position decoder signal, is sent into commutator module which generates Hpwm-Lon mode of pulse modulation waves, according to rotor position decoding (Table 2) and commutation rule (Table 3) to control ordered switching of the inverter's IGBT full bridge circuits. This driving mode is an output mode with high leg PWM modulation and low leg constant live. It can suppress motor torque ripple and improve system dynamic performance [21]. Details of each subsystem are shown in Figures 9–13.

From the six switching states of the homopolar motor upon commutation, we note that the motor's commutation sequence is associated with the rotor position. According to the motor's operational principle, when the motor rotates clockwise, the switching relationship between the rotor position and the switching tube is given in Table 2. The switching tube's conducting state is set to "1", while its breaking state is set to "0".

6. Simulation Result and Analysis

Acceleration energy storage is one of the core issues of system control and relates to system's energy storing speed and safety. When energy storing acceleration is controlled, the flywheel motor runs as an electric motor [17]. In this paper, the parameters required by the homopolar motor and controller were set in a homopolar motor control system model which was built on the "simulation model editor" interface on software platform Matlab, see Table 4.

In order to test each performance index of the system after all module parameter settings of the homopolar motor control system and the corresponding program file embeddings were completed, we repeated system running, simulation, and tuning again and again and finally obtained the simulation result and made a necessary analysis of the tuning result and waveform.

In the simulation experiment of tuning the homopolar motor control system, in order to ensure the motor's safe startup and simulate some practical factors in its real environment, the motor started with a load (0.1 N·m) at the initial preset speed of $n^* = 15000$ r/min. At 0.5 S it added an external load $TL = 0.4$ N·m and continued to operate. The speed response wave is as shown in Figure 14.

Figure 14 shows that the motor quickly accelerates to 15,000 r/min after the start-up, with a little speed overshoot at the beginning, yet $\sigma\% < 0.04\%$, acceleration time $t_p = 0.137$ S, and transition time $t_s = 0.23$ s, with very small and negligible static error. At 0.5 S, the motor begins to run with load ($TL = 0.4$ N·m) and slightly slows but maintains basically at 15,000 r/min. The whole system responds fast and runs steadily. Eventually, the motor speed is basically stable at the set value with little fluctuation.

Other performance indexes of the motor: Figure 15 is the torque wave of the electric motor. At 0.137 S, the torque is basically stable at 2.1 N·m but with notable fluctuation.

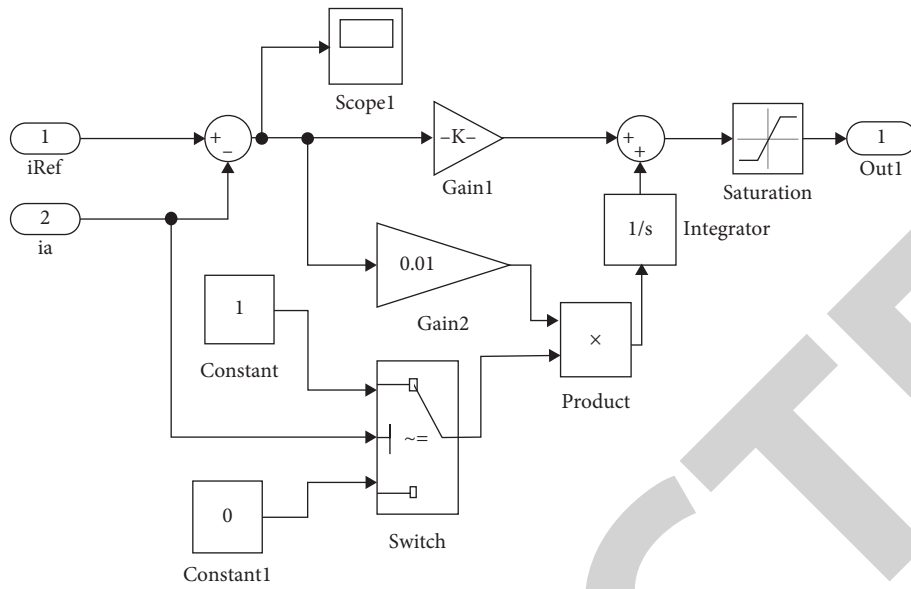


FIGURE 10: Subsystem simulation model of current controller PI-current.

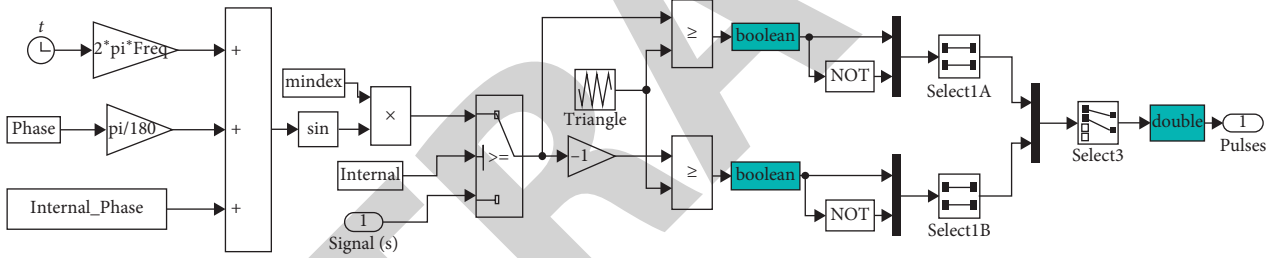


FIGURE 11: Subsystem simulation model of the PWM generator.

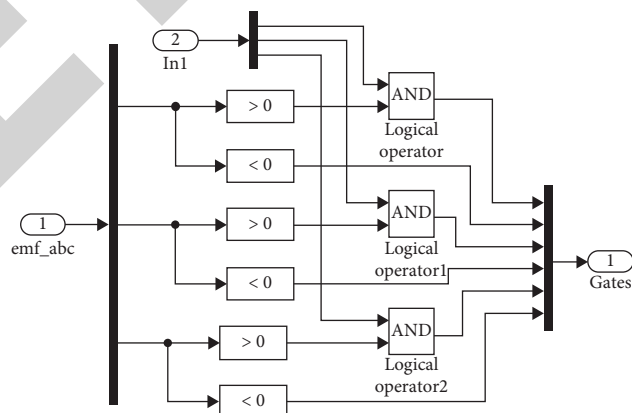


FIGURE 12: Subsystem simulation model of the commutator.

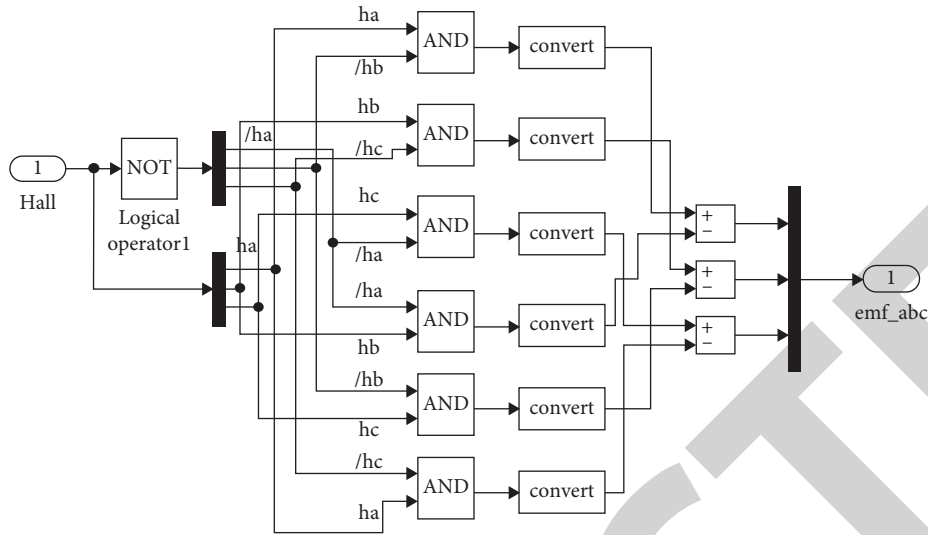


FIGURE 13: Subsystem simulation model of the decoder.

TABLE 4: Parameter list of the homopolar motor control system.

Homopolar motor	Stator resistance $R_s = 0.055 \Omega$ Stator inductance $L_s = 0.000115H$ Moment of inertia $J = 5.615 \times 10^{-3} kg \cdot m^2$ System viscous damping $10^{-3} N \cdot ms$	Constant torque $0.047 N \cdot m/A$ Static friction $0.4 N \cdot m$ Number of pole pairs $p = 4$ Rated speed 8000 rpm
PI speed controller	$K_p = 2$	$K_i = 0.01$
Current PI controller	$K_p = 0.25$	$K_i = 0.01$

<Speed waveform of PI control of Homopolar motor>

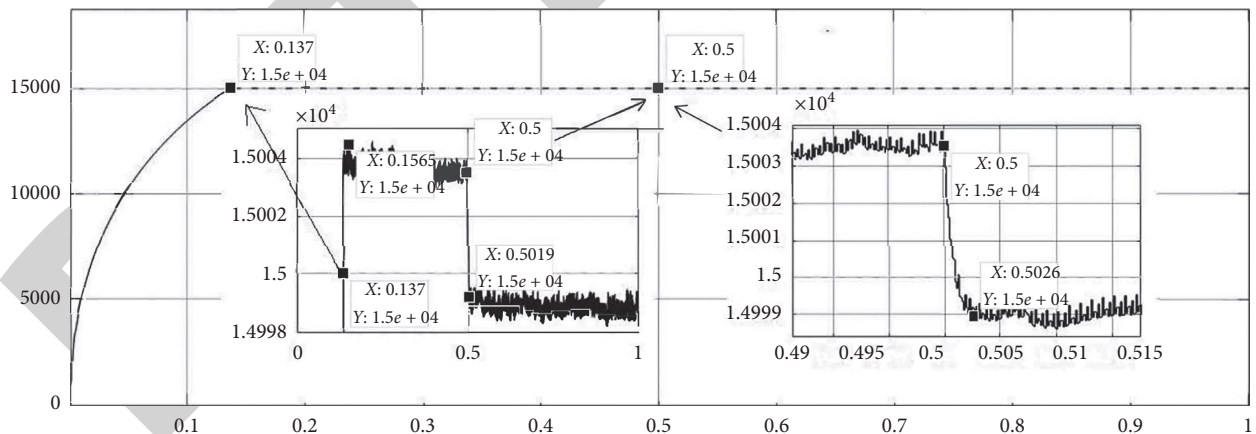


FIGURE 14: Speed waveform of PI control of homopolar motor.

When the motor runs with load at 0.5 S, the torque changes to 2.5 N·m. The pulse wave output by the commutator is PWM signal in Hpwm-Lon modulation mode (see Figure 16). Figure 17 is the induction electromotive force of three-phase motor stator. The stator's induction electromotive force is in the form of 180° trapezoidal wave and each corresponding phase of the magnetic flux is also in

trapezoidal waveform, so this system is also known as the speed-governing system of trapezoidal-wave permanent magnet synchronous motor (TPMSM). Figure 18 is the induced current waveform of the three-phase motor stator. The motor current is in 120° rectangular waveform. As the voltage adopts PWM chopper control, the rectangular wave contains a significant harmonic component. Upon the

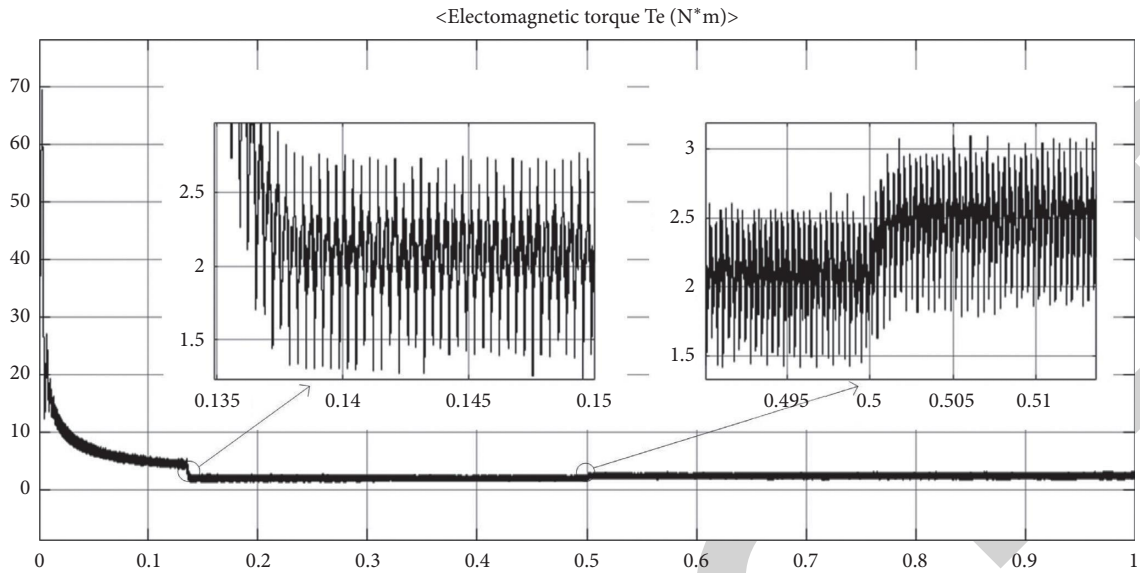


FIGURE 15: Torque waveform of the homopolar motor of PI control.

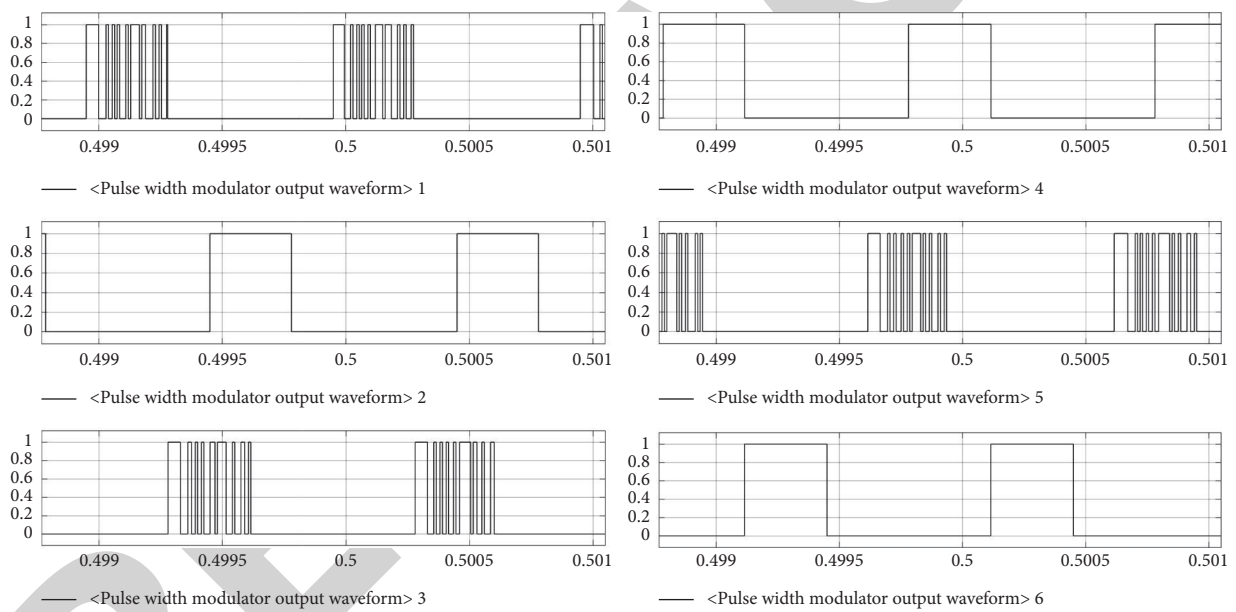


FIGURE 16: Pulse width modulator output waveform of the Homopolar motor of PI control.

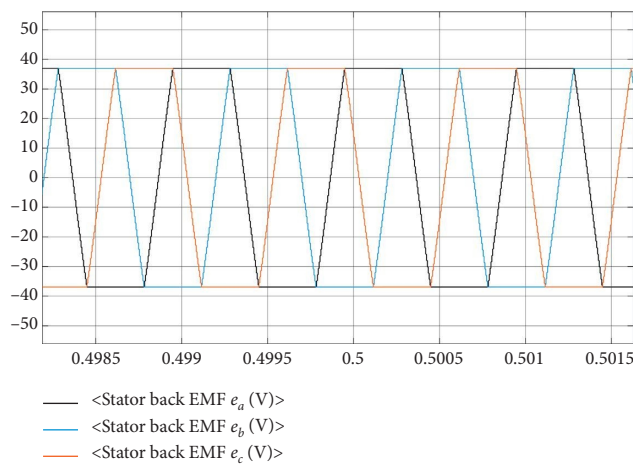


FIGURE 17: Three-phase-induced electromotive force waveform of the homopolar motor of PI control.

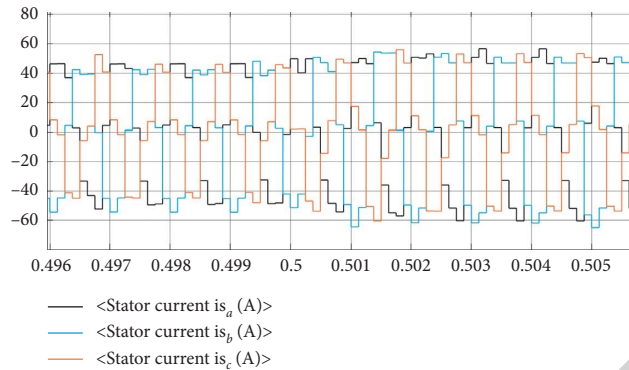


FIGURE 18: Three-phase-induced current waveform of the homopolar motor of PI control.

loading at 0.5 S, the state of the power switching tube of the PWM modulator changes and causes the current pulse amplitude to vary slightly.

It is thus clear that the simulation result basically coincides with the expected result, which suggests that the control method is feasible. The purpose of this research, however, is only to verify the correctness and feasibility of this control method by simulation and analysis considering the large inertia of flywheel and long acceleration time in the practical control of flywheel motor acceleration. The experiment result and the discussion part of work apply to general parameters and to the parameters used in experiment.

7. Conclusion

Flywheel energy storage will be a future direction for the field of energy saving, though traditional flywheel motors have the defects of great iron loss in rotation, poor rotor strength, and robustness. In view of these problems, the electrically excited homopolar motor is adopted for flywheel energy storage in this research for its advantages such as simple structure, high rotor strength, and low iron loss in high-speed rotation. A PI-controlled double closed-loop governing system of the homopolar motor was designed on simulation platform Simulink. And the charging process of the flywheel energy storage is studied in this paper. The simulation result shows that the control system of the electrically excited homopolar motor realized the regulating of motor phase current and torque by modulating PWM duty cycle in Hpwm-Lon mode with a speed-current controller using PID control strategy, realized fast speed governing, showed good static and dynamic performances, and achieved the purpose of quick charge by flywheel energy storage. This research is just a small part of the flywheel energy storage project which will continue the research and verification of the energy storage and discharge process later, use advanced motor intelligent control algorithm to realize homopolar motor's robust control, reduce the switching loss and torque ripple, and further improve the system performance.

Data Availability

The data used to support the findings of this study are available from the corresponding author upon request.

Disclosure

We confirm that the content of the manuscript has not been published or submitted for publication elsewhere.

Conflicts of Interest

The authors declare that there are no conflicts of interest.

Authors' Contributions

All authors have read and approved the final version of the manuscript.

Acknowledgments

We would like to thank my mentor Professor Dong for stimulating discussions with respect to the topic of this paper and laboratory equipment. This research was supported by Inner Mongolia Autonomous Region Natural Science Foundation (2017MS0521) and Research Program of Science and Technology at Universities of Inner Mongolia Autonomous Region (NJZY17352 and NJZY18232).

References

- [1] S. Koohi-Fayegh and M. A. Rosen, "A review of energy storage types, applications and recent developments," *Journal of Energy Storage*, vol. 27, p. 101047, 2020.
- [2] B. H. Kenny, P. E. Kascak, R. Jansen, T. Dever, and W. Santiago, "Control of a high-speed flywheel system for energy storage in space applications," *IEEE Transactions on Industry Applications*, vol. 41, no. 4, pp. 1029–1038, 2005.
- [3] I. Alan and T. A. Lipo, "Induction machine based flywheel energy storage system," *IEEE Transactions on Aerospace and Electronic Systems*, vol. 39, no. 1, pp. 151–163, 2003.
- [4] Z. Wang and X. Xue, "A Type of electrically-excited homopolar rotary motor," pp. 4–3, Beijing, China, 2018, Patent no: CN107872104A.
- [5] Z. Lou, K. Yu, L. Wang, Z.-A. Ren, and C. Ye, "Two-reaction theory of homopolar inductor alternator," *IEEE Transactions on Energy Conversion*, vol. 25, no. 3, pp. 677–679, 2010.
- [6] Q. Xin, K. Yu, Z. A. Ren, Z. lou, and C. ye, "Inductance mathematic model of a homopolar inductor alternator in a novel pulse capacitor charge power supply," *IEEE Transactions on Plasma Science*, vol. 41, no. 5, pp. 1231–1236, 2013.

- [7] D. Stephen, X. Liu, S. Su et al., *Electric Machinery*, Publishing House of Electronics Industry, Beijing, China, 7th edition, 2016.
- [8] K. J. Astrom and T. Haggglund, *PID controllers : Theory Design and Tuning*, Instrument Society of America, Research Triangle Park, NC, USA, 2nd edition, 1995.
- [9] P.-D. Yang, *PID Controller Parameters Tuning Method and its Application*, China Electric Power Press, Beijing, China, 2016.
- [10] Z. He, *Parameters Tuning of PID Controller and It's Application*, Zhejiang University, Zhejiang, China, 2005.
- [11] A. Visioli and Q. Zhong, *Smith-principle-based PID-type Control*, Springer, Berlin, Germany, 2011.
- [12] I. Boiko, *Discontinuous Control Systems*, Birkhuser, Cambridge, MA, USA, 2009.
- [13] S. Manesis and N. George, *Introduction to Industrial Automation*, Taylor and Francis, Milton Park, UK, 2018.
- [14] G. P. Liu, *Control Systems Design*, Springer, Berlin Germany, 2005.
- [15] Birkhuser, *The Servo Problem in Discontinuous Control systems*, Birkhuser, Cambridge, MA, USA, 2009.
- [16] L. Ibarra and C. Webb, *Advantages of Fuzzy Control While Dealing With Complex/Unknown Model Dynamics: A Quadcopter Example*, IntechOpen, London, UK, 2016.
- [17] P. Tang, *Research on Magnetic Suspension Flywheel Electric Machine for Energy Storage and Control of Drive Systeem*, Harbin Institute of Technology, Harbin, China, 2009.
- [18] E. Sghaier, A. Bourdon, D. Remond, J.-L. Dion, and N. Peyret, *Dynamic Behavior of Very-High Speed Rotors at Non-stationary Conditions*, Springer International Publishing, Manhattan, NY, USA, 2018.
- [19] L. Jing, X. Xue, and N. Yang, "Research on fuzzy PID control strategy for double closed-loop control system of brushless DC motor," *Revista de la Facultad de Ingenieria*, vol. 9, pp. 8–14, 2017.
- [20] L. Jing and N. Yang, "Research on Switching PID control strategy for brushless direct current motor," *Boletin Tecnico/ Technlcal Bulletin*, vol. 55, pp. 676–683, 2017.
- [21] Q. Li, H. Huang, and B. Yin, "The study of PWM methods in permanent magnet brushless DC motor speed control system," in *Proceedings of the International Conference on Electrical Machines and Systems*, pp. 3897–3900, Wuhan, China, October 2008.